

# Studies on the Thermal Stability and Degradation Kinetics of Pd/PC Nanocomposites

Valmikanathan P. Onbattuveli,<sup>1</sup> Willie E. Rochefort,<sup>1</sup> John Simonsen,<sup>1</sup> Seong-Jin Park,<sup>2</sup> Randall M. German,<sup>3</sup> Sundar V. Atre<sup>1</sup>

<sup>1</sup>Oregon Nanoscience and Microtechnologies Institute, Oregon State University, Corvallis, Oregon

<sup>2</sup>Department of Mechanical Engineering, Pohang University of Science and Technology, Pohang, Republic of Korea

<sup>3</sup>Department of Mechanical Engineering, San Diego State University, San Diego, California

Received 6 November 2008; accepted 11 January 2009

DOI 10.1002/app.32403

Published online 15 July 2010 in Wiley InterScience (www.interscience.wiley.com).

**ABSTRACT:** Effect of heating rate, Pd content, and synthesis method on the thermal stability of the *ex situ* and *in situ* Palladium/polycarbonate (Pd/PC) nanocomposites was investigated. TEM images revealed discrete Pd nanoclusters of about 5 and 15 nm sizes for 1 and 2 vol % *ex situ* nanocomposites, respectively. However, agglomerated Pd nanoclusters were noticed in the *in situ* samples, irrespective of the Pd content. The *ex situ* Pd/PC nanocomposites showed high onset temperature ( $T_i$ ) for thermal degradation of PC than the *in situ* and pure PC samples. Pd content and heating rates were found to have a positive influence on the  $T_i$  and  $T_m$  (temperature at the maximum degradation rate occurs) of the Pd/PC nanocomposites. Thermal degradation

of the PC was found to follow the first-order kinetics in the Pd/PC nanocomposites. The activation energies associated with the degradation were determined by using the Kissinger method. These activation energies are used to construct the Master decomposition curve (MDC) and weight–time–temperature ( $\alpha$ - $t$ - $T$ ) plots that describe the time-temperature dependence of the PC pyrolysis in the Pd/PC nanocomposites. These constructed  $\alpha$ - $t$ - $T$  plots were validated with the data from isothermal measurements. © 2010 Wiley Periodicals, Inc. *J Appl Polym Sci* 118: 3602–3611, 2010

**Key words:** palladium/polycarbonate nanocomposites; activation energy; degradation kinetics

## INTRODUCTION

Using polymers with metal nanoparticles can result in nanocomposites with a wide range of useful characteristics.<sup>1</sup> For example, palladium nanoparticles dispersed in polymers find useful applications as sensors and catalysts.<sup>2–4</sup> In these applications, it is important to understand the thermal stability of the polymer nanocomposites so as to determine their useful operating temperature limits.

There are two different approaches to synthesize metal/polymer nanocomposites: *in situ* and *ex situ*. The *ex situ* methods generally involve the addition of metal nanoclusters to the polymer matrix.<sup>5,6</sup> On the other hand, the *in situ* methods involve the preparation of nanoclusters in the presence of a polymer or polymerization in the presence of nanoclusters.<sup>7,8</sup> Prior studies have been reported that these approaches offer a greater possibility of synthesizing nanocomposites with useful thermal,<sup>5,9,10</sup> optical,<sup>11,12</sup> and electrical properties.<sup>13,14</sup>

In this study, the degradation behavior of the pure polycarbonate (PC) and palladium/polycarbon-

ate (Pd/PC) nanocomposites under N<sub>2</sub> atmosphere was studied using the thermogravimetric analysis (TGA). The influences of the heating rates, Pd content, and mode of synthesis (*in situ* and *ex situ*) on the degradation temperatures were determined. The activation energies associated with the thermal degradation of these nanocomposites were calculated from TGA data using the Kissinger method. The master decomposition curve (MDC) and weight-time-temperature ( $\alpha$ - $t$ - $T$ ) plots for the samples were subsequently formulated based on the activation energies and rate constant calculated by the Kissinger method. The  $\alpha$ - $t$ - $T$  plots to the experimental values were compared with the data from isothermal measurements.

## EXPERIMENTAL

### Materials

Palladium chloride (PdCl<sub>2</sub>), conc. hydrochloric acid (HCl), and dichloromethane (CH<sub>2</sub>Cl<sub>2</sub>) were purchased from Merck, India. Sodium borohydride (NaBH<sub>4</sub>) and dodecanethiol (C<sub>12</sub>H<sub>25</sub>SH) were purchased from Aldrich, USA. Polycarbonate (Caliber T303; molecular weight  $M_w$  of 160,000) was obtained from Dow Chemicals, USA. Deionized water with a resistivity of  $18 \times 10^6 \Omega \text{ cm}$  was obtained from a Millipore unit.

Correspondence to: S. V. Atre (sundar.atre@oregonstate.edu).

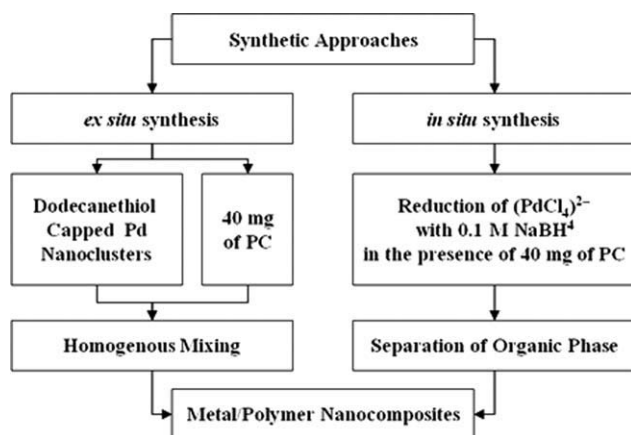


**Figure 1** Schematic representation of synthetic approaches for preparing *ex situ* and *in situ* Pd/PC nanocomposites.

### Synthesis of Pd/PC nanocomposite films

The two methods of nanocomposite synthesis of Pd/PC that were used in this study are shown in Figure 1.

- *Ex situ* method:  $C_{12}H_{25}SH$ -protected Pd nanoclusters were prepared using the Brust method.<sup>15</sup> The Pd nanoclusters were then homogeneously mixed with a solution of 40 mg of PC in 20 mL of  $CH_2Cl_2$  followed by film casting at room temperature.
- *In situ* method: PC (40 mg) was dissolved in  $CH_2Cl_2$  (20 mL). 15 mg (for 2 vol %) and 7.5 mg (for 1 vol %) of  $PdCl_2$  was first dissolved in 2 mL of concentrated HCl so as to form a complex  $[PdCl_4]^{2-}$ , and was further dissolved in 48 mL water to form a 1 mM solution. This biphasic mixture was stirred continuously using a magnetic stirrer for 30 min. A freshly prepared solution of  $NaBH_4$  in 20 mL water (0.1 M) was added drop-wise to the mixture. The color of the reaction mixture changed rapidly from golden yellow to black, indicating the formation of Pd nanoclusters. After stirring for 3 h, the organic phase was separated, washed with water, and was directly cast into film at room temperature. Following reduction, the Pd nanoparticles get transferred from the aqueous phase to the organic phase.<sup>16</sup>

### Characterization of Pd/PC nanocomposite films

TEM micrographs were taken on a JEOL model 1200 EX instrument operated at an accelerating voltage of 120 kV. Samples for TEM analysis were of a stock solution of 0.5 mL of 1 wt % nanocomposite solution in dichloromethane. These stock solutions were cast on a carbon coated Cu grid (400 mesh) and dried

slowly at room temperature. TGA was performed using TA instruments thermal analysis system. The instrument operated under  $N_2$  atmosphere at a purge rate of 50 mL/min. All TGA measurements were carried out in the temperature range of 30 to 900°C with heating rates of 5, 10, 15, and 20°C/minute. All isothermal measurements were done at 450°C for 1 h under the same  $N_2$  atmosphere.

## RESULTS AND DISCUSSION

### Morphology of Pd/PC nanocomposites

The TEM images of the *ex situ* nanocomposites with 1 and 2 vol % Pd (on a stoichiometric basis) revealed dispersed Pd nanoclusters of about 5 and 15 nm embedded in PC matrix (Fig. 2a,b). The decrease in nanocluster size is attributed to the higher metal salt: thiol ratio in the case of the 2 vol % Pd sample. Based on earlier reports on the synthesis and morphology of *n*-alkanethiol-protected Pd nanoclusters,<sup>17,18</sup> the presence of dodecanethiol on the surface of the Pd nanoclusters in this study is likely to ensure the separation of the nanoclusters even after mixing with PC. However, the average particle size of the Pd nanoclusters in previous studies was found to be below 5 nm size; using the Brust method.<sup>15</sup> Although similar range of metal salt: thiol ratio and reducing agent were used in this study, an increase in the size of the nanoclusters was found. This was confirmed to be at least partly due to the absence of the surfactant, tetraoctyl ammonium bromide, in the reaction mixture, which helps in phase transfer of reduced Pd nanoclusters. The effect of increased temperature of the reaction mixture from ice-cold condition in the earlier studies in comparison to the reaction room temperature may have also contributed to the increased size of the nanoclusters.<sup>19</sup> Alternatively, a difference in the concentration of reducing agent may have also contributed to the increase in the average size of nanoclusters.

In contrast to the above system, the *in situ* nanocomposites of Pd nanoclusters (1 and 2 vol % on a stoichiometric basis) in PC showed significant

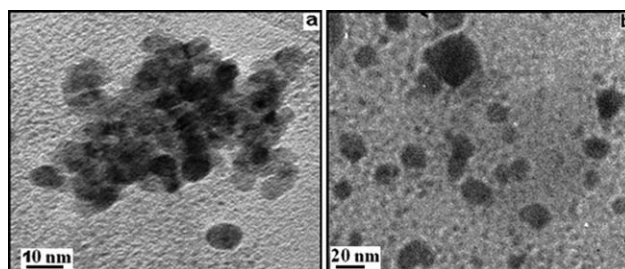


**Figure 2** TEM images of *ex situ* nanocomposites revealing dispersed Pd nanoclusters of about 10 nm for (a) 1 vol % and (b) 2 vol % nanocomposites.

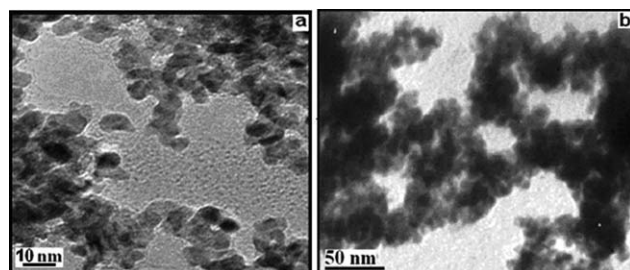


**Figure 3** TEM images of *in situ* nanocomposites revealing agglomerated Pd nanoclusters for (a) 1 vol % and (b) 2 vol % nanocomposites.

agglomeration (Fig. 3a,b). Similar observations on agglomeration were reported by Chen et al. using Pd with mercapto-poly(ethylene glycol),<sup>20</sup> and Chatterjee et al. with Au with poly(dimethylamino ethyl methacrylate-*b*-methyl methacrylate) copolymers ( $M_w$ : 50,000).<sup>21</sup> However, discrete nanoclusters were also noted by Khanna et al.<sup>22</sup> in system of Ag with poly(vinyl alcohol) ( $M_w$ : 125,000, nanocluster size: about 10 nm). Thus, morphological changes in nanocomposites appear to be strongly dependent on the specific polymer systems and reaction conditions.

Wang et al. have suggested that to obtain discrete nanoclusters, the rate of adsorption of organic ligands on the surface of nanoclusters should equal the rate of nanocluster formation.<sup>23</sup> Accordingly, organic ligands with lower molecular weight have generally been found to be more effective in limiting the nanoclusters size.<sup>23,24</sup> The wide-ranging behavior of agglomeration in nanocomposites prepared by the *in situ* methods may also be due to the differences in the conformations of the polymer chain in the different studies. These conformational differences can arise from variations in molecular weight, solvent, and temperature. Consequently, the mobility of the polymer during adsorption on the nanocluster surface can be affected, thereby limiting the agglomeration of the nanoclusters. In addition, the nature of interactions between the polymer and the surface of the nanoclusters may also play a role in determining the morphology of the resulting nanocomposites. Further studies are needed to better understand the differences in morphologies observed between the *in situ* and *ex situ* nanocomposites. The following sections examine the consequences of the differences in morphology on the thermal properties of the nanocomposites.

### Thermal stability

The TGA curves for the pure PC and the Pd/PC nanocomposites at different heating rates are shown in the Figure 4. For each sample, the corresponding plots for the rate of weight loss with respect to temperature in the Figure 5 revealed the temperature at which the maximum rate of weight loss ( $T_m$ )

occurred. In Figure 5, the plots for the rate of weight with respect to temperature are represented with normalized weight  $\alpha$  which can be expressed as,

$$\alpha = \frac{W_T - W_f}{W_i - W_f} \quad (1)$$

where  $W_T$  is the weight of the sample at the given temperature,  $W_i$  is the weight at the starting of TGA experiment, and  $W_f$  is the weight at the ending of TGA experiment. The onset temperature of degradation ( $T_i$ ) and the end temperature of degradation ( $T_f$ ) can be obtained from the TGA. The difference  $\Delta T = (T_f - T_i)$ , represents the temperature range for thermal degradation of a given sample. The ratio of  $\Delta T$  with the heating rates ( $r$ ) gives the overall degradation time ( $\Delta T/r$ ) of the sample. The  $T_m$ ,  $T_i$ ,  $T_f$ ,  $\Delta T$ , and  $\Delta T/r$  of the pure PC and the Pd/PC nanocomposites are listed in Table I. The table also includes the average residual (wt %) remaining after the TGA runs for each sample. On a stoichiometric basis, 1 and 2 vol % of Pd nanoclusters equals 9.2 and 18.4 wt %, respectively. Thus, the residual exceeding these values for the respective samples could account for the incomplete thermal degradation of samples under  $N_2$  atmosphere.

### Effect of heating rate

As seen in Table I, the thermal stability of pure PC and the Pd/PC nanocomposites increased with increase in the heating rates. The results are supported by the shifts in the values of  $T_i$ ,  $T_f$ , and  $T_m$  to the higher range with increase in the heating rates. Also, the overall degradation time ( $\Delta t_d = \Delta T/r$ ) for the sample decreases with increase in the heating rates. Similar results were obtained by Peng et al.<sup>10</sup> for polyvinyl alcohol/silica nanocomposites.

The degradation of a polymer chain typically commences with the formation of the free radicals, which then transfer to adjacent chains via intermolecular collisions, ending with the termination step. However, in this study, the Pd nanoclusters could reduce the frequency of collisions between the PC chains and thus suppress the mobility of the radicals. A similar behavior by the metal nanoparticles was noticed by Lee et al. in the Pd/polystyrene and Pt/polystyrene systems.<sup>25</sup> Thus, with the addition of Pd nanoclusters enhancing the thermal stability, further studies on the factors like the morphology and content of the nanoclusters in the polymer matrix could be important.

### Effect of Pd amount

From Figure 4 and Table I, an increase in the Pd content in the nanocomposites, results in an increase in the  $T_i$ ,  $T_f$ , and  $T_m$ . But no particular trend is noticed with these increments. Similar results were obtained

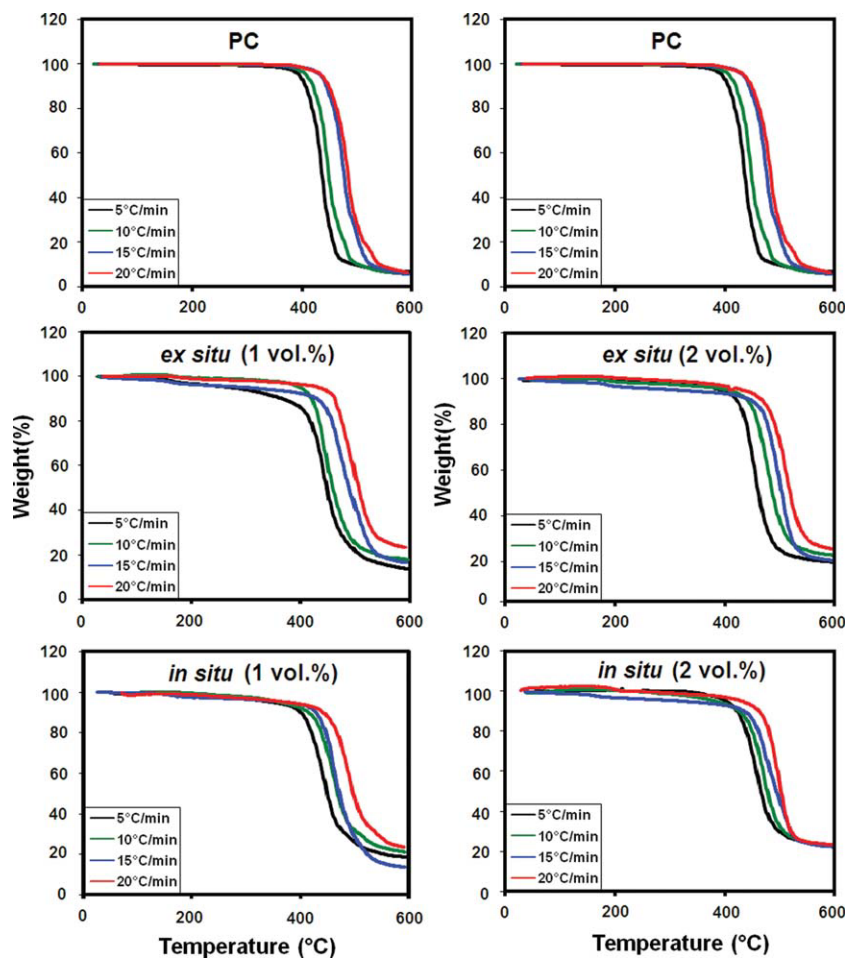


**Figure 4** TGA for pure PC and Pd/PC nanocomposites with (a) 1 vol % and (b) 2 vol % Pd at different heating rates (5, 10, 15, and 20°C/min). [Color figure can be viewed in the online issue, which is available at [www.interscience.wiley.com](http://www.interscience.wiley.com).]

by Xia et al.<sup>5</sup> for Cu/polyethylene (Cu content: 17 wt %), Aymonier et al.<sup>7</sup> for Pd/ polymethyl methacrylate (Pd content: 0.01 vol %) and Hsu et al.<sup>9</sup> for Au/polyurethane (Au content: 0.065 wt %). However, such proportional increment in the thermal stability of the nanocomposites was not found to be a common aspect. For example, Lee et al.<sup>25</sup> found no further increment in the thermal stability Pd/PS nanocomposites when the Pd content is doubled. In our case, the relationship between the Pd content and the thermal stability can possibly be explained as the outcome of the suppressed PC chain collisions. Further research is required to determine the critical limit up to which this trend may be followed.

#### Effect of synthesis method

As mentioned earlier, another factor to be noted with regard to Pd nanoclusters is their morphology. Aymonier et al.<sup>7</sup> and Hsu et al.<sup>9</sup> observed that the thermal stability of the nanocomposites increase with decrease in particle size and agglomeration. In this study, Pd/PC nanocomposites with discrete (*ex situ*)

and agglomerated (*in situ*) were tested. It can be seen from Table I that any *ex situ* nanocomposite is more thermally stable than the *in situ* ones with equal or less Pd content. A similar increase in thermal stability was noted in earlier reports by Huang et al.<sup>26</sup> for Au/poly(methyl styrene) with particle size of 3.5 nm, Aymonier et al.<sup>7</sup> for Pd/PMMA with particle size of 2.5 nm, and Hsu et al.<sup>9</sup> for Au/polyurethane with particle size of 5 nm. These results roughly correlate with changes in the area of the polymer-nanoclusters interface. The TEM images (Fig. 2) show that the *ex-situ* nanocomposites with discrete Pd nanoclusters will have a higher interfacial area than the *in situ* nanocomposites with highly agglomerated nanoclusters. Thus, the Pd nanoclusters in *ex situ* samples may suppress the chain collisions more effectively leading to higher thermal stability.

#### Degradation kinetic studies

Kissinger method for obtaining activation energy

The TGA curves showed that the thermal degradation of the Pd/PC nanocomposites was a single

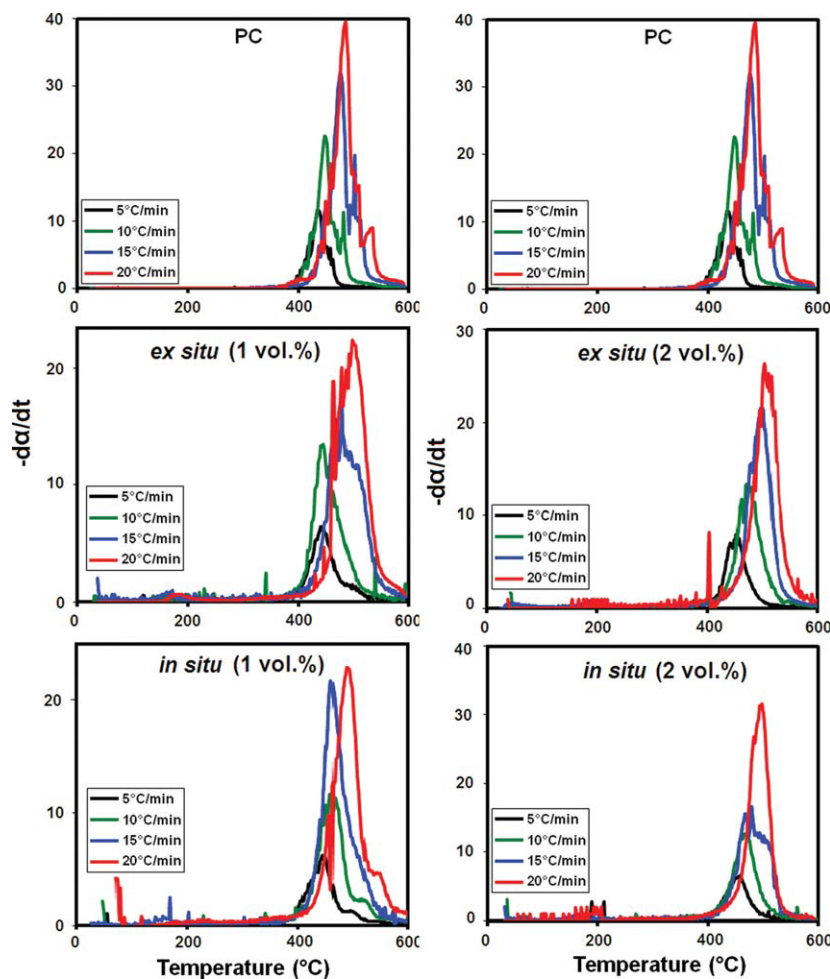


**Figure 5** Plots for the rate of weight with respect to temperature for pure PC and Pd/PC nanocomposites with (a) 1 vol % and (b) 2 vol % Pd at different heating rates (5, 10, 15, and 20°C/min). [Color figure can be viewed in the online issue, which is available at [www.interscience.wiley.com](http://www.interscience.wiley.com).]

**TABLE I**  
Characteristic Temperatures for the Degradation of Pure PC and the Pd/PC Nanocomposites TGA-Tested Under N<sub>2</sub> Atmosphere

Sample	$r$ (°C/min)	$T_i$ (°C)	$T_f$ (°C)	$\Delta T$ (°C)	$\Delta t_d$ (min)	$T_m$ (°C)	Residual (wt %)
Pure PC	5	376	482	106	21.2	434	16.8 ± 3.9
	10	392	508	116	11.6	442	
	15	430	538	108	7.2	476	
	20	434	554	120	6.0	486	
1 vol % <i>ex situ</i>	5	392	502	110	22.0	442	18.1 ± 4.8
	10	416	518	102	10.2	446	
	15	434	556	122	8.1	480	
	20	452	570	118	5.9	498	
1 vol % <i>in situ</i>	5	392	522	130	26.0	446	20.6 ± 1.9
	10	404	544	140	14.0	460	
	15	432	558	126	8.4	462	
	20	440	580	140	7.0	490	
2 vol % <i>ex situ</i>	5	406	514	108	21.6	454	22.6 ± 2.7
	10	422	540	116	11.6	472	
	15	448	556	108	7.2	498	
	20	468	576	108	5.4	504	
2 vol % <i>in situ</i>	5	398	516	118	23.6	460	22.7 ± 0.7
	10	420	524	104	10.4	468	
	15	434	556	122	8.1	480	
	20	452	556	104	5.2	498	

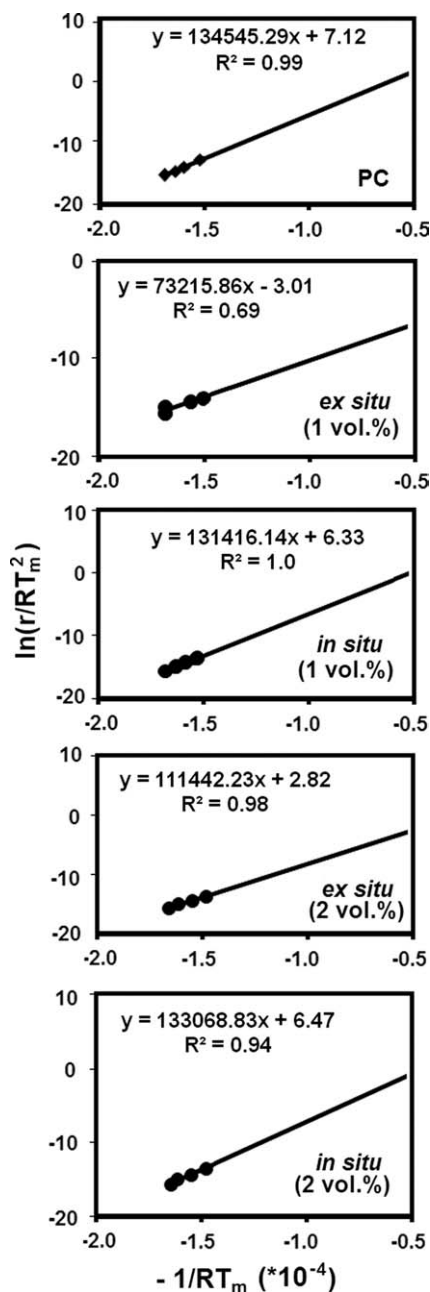


**Figure 6** Determination of activation energies for samples tested by the Kissinger method.

stage process following a first order reaction kinetics for their thermal degradation. Similar observations were made by Krkljes et al. on Ag/polyvinyl alcohol,<sup>27</sup> Aymonier et al. on Pd/polymethyl methacrylate,<sup>7</sup> and Hsu et al. on Au/polyurethane.<sup>9</sup> The remaining weight fraction ( $\alpha$ ) of a sample in a TGA experiment, can be expressed as:

$$\frac{d\alpha}{dt} = -K\alpha \quad (2)$$

where  $t$  is the time and  $K$  is the rate constant for thermal degradation which follows the Arrhenius equation:

$$K = k_0 \exp\left[-\frac{Q}{RT}\right] \quad (3)$$

where  $k_0$  is the rate constant parameter,  $Q$  is the activation energy,  $R$  is the universal gas constant, and  $T$  is the temperature. By substituting, eq. (3) into eq. (2), then the following equation is obtained:

$$\frac{d\alpha}{dt} = -\alpha k_0 \exp\left[-\frac{Q}{RT}\right] \quad (4)$$

The activation energy  $Q$  for the Pd/PC nanocomposites degradation can be determined from TGA and for the rate of weight with respect to temperature data in a method developed by Kissinger.<sup>28</sup> The Kissinger method utilizes the temperature  $T_m$  at various heating rates as follows:

$$\frac{d}{dt}\left(-\frac{d\alpha}{dt}\right) = 0 \text{ at } T = T_m. \quad (5)$$

In a given TGA, the weight ( $\alpha$ ), as well as the temperature ( $T$ ) depends on the time ( $t$ ), and, thus, the above differentiation can be expressed as,

$$\frac{rQ}{RT_m^2} = k_0 \exp\left[-\frac{Q}{RT_m}\right]. \quad (6)$$

with the condition of constant heating rate  $r$ , that is  $dT/dt = r$ .

By plotting a graph between  $\ln(r/T_m^2)$  and  $-1/RT_m$  from several different heating rates can be plotted, the apparent activation energy  $Q$  can be calculated from the slope of this plot, as shown in Figure 6. The rate constant  $k_0$  can be back-calculated from the intercept value. The values of  $Q$  and  $k_0$  are tabulated in Table II.

The activation energy of pure PC was calculated to be 135 kJ/mol. In comparison, an activation energy of 165 kJ/mol reported by Polli et al. using the Vyazovkin model and the free kinetics method.<sup>29</sup> As seen from Table II, addition of Pd nanoclusters into the polymer matrix reduced the  $k_0$  values for the *in situ* as well as the *ex situ* nanocomposites. However, the  $Q$  values for the *ex situ* nanocomposites

**TABLE II**  
Activation Energy ( $Q$ ) and Rate Constant ( $k_0$ ) for the Degradation of Pure PC and the Pd/PC Nanocomposites Along with the  $R^2$  Values

Sample	$Q$ (kJ/mol)	$R^2$	$k_0$ ( $s^{-1}$ )	$R^2$
Pure PC	135	0.99	$1.4 \times 10^7$	0.97
1 vol % <i>ex situ</i>	73	0.69	$3.0 \times 10^2$	1.00
1 vol % <i>in situ</i>	131	1.00	$5.3 \times 10^4$	0.99
2 vol % <i>ex situ</i>	111	0.98	$9.3 \times 10^4$	0.96
2 vol % <i>in situ</i>	133	0.94	$6.3 \times 10^6$	0.97

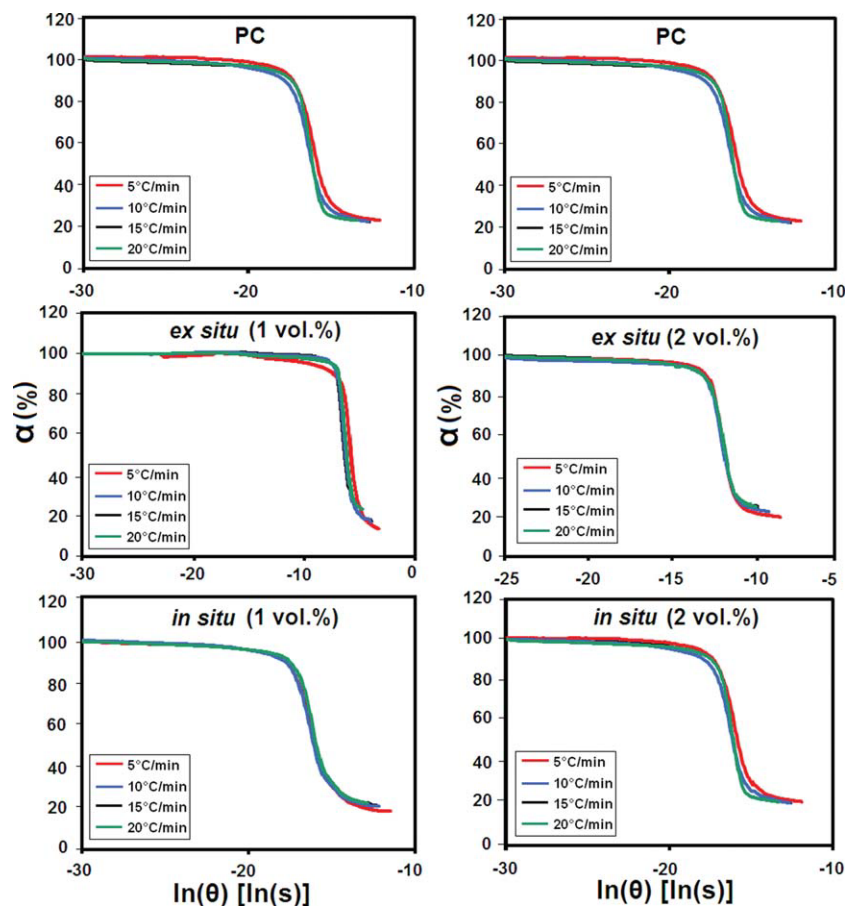


**Figure 7** MDCs for pure PC and Pd/PC nanocomposites with (a) 1 vol % and (b) 2 vol % Pd. [Color figure can be viewed in the online issue, which is available at [www.interscience.wiley.com](http://www.interscience.wiley.com).]

were lower than for the *in situ* nanocomposites which were largely unchanged relative to the unfilled PC. Similar results were reported by Lee et al.<sup>25</sup> in Pd/polystyrene systems. Further in the case of the *ex situ* nanocomposites, a lower value of  $Q$  was observed for the 1 vol % Pd system relative to the 2 vol % Pd system. Variations in the  $Q$  and  $k_0$  values among the 1 and 2 vol % Pd *ex situ* samples could be due to the variations in the particle size of the Pd nanoclusters.

Based on the decreased  $Q$  values for Pd/PC nanocomposites in Table II, the Pd nanoclusters could be expected to catalyze the thermal degradation of the nanocomposites. Instead, the increase in the thermal stability is possibly due to the decreased rate constant parameters  $k_0$ . Lee et al. state that  $k_0$  values directly correspond to the collision frequency of the polymer chains.<sup>25</sup> For a given Pd content, the smaller Pd nanoclusters due to their higher surface area can suppress the chain collisions and thus reduce the degradation rate. This may partially be a possible reason for the differences in the  $k_0$  values of the Pd/PC nanocomposites in comparison to the unfilled PC. However, further experiments are needed to understand the trends in  $k_0$  as a function

of concentration and morphology of the Pd nanoclusters in the PC matrix.

#### Master decomposition curve

TGA plots and plots for the rate of weight loss with respect to temperature can be referred to determine the thermal stability of the nanocomposites. However, a difficulty arises in referring to these plots in the case of predicting the useful life of a sensor or catalyst operating at varying working combinations of temperature and time. The master decomposition curve (MDC) methodology is generally used to construct a systematic plot for several time-temperature cycles with a given polymeric material. These MDC curves are formulated based on the intrinsic kinetics of polymer pyrolysis based on the method of DiAntonio et al.<sup>30</sup> Typically, the TGA curves of polymer degradation follow a single sigmoid path. However, multi-component systems may have two or more sigmoids due to the different molecular weights and degradation paths of various polymer components.<sup>31</sup> In our case, even though being a two-component system, the Pd/PC nanocomposites showed a single sigmoid path. Degradation of Pd into its oxides is

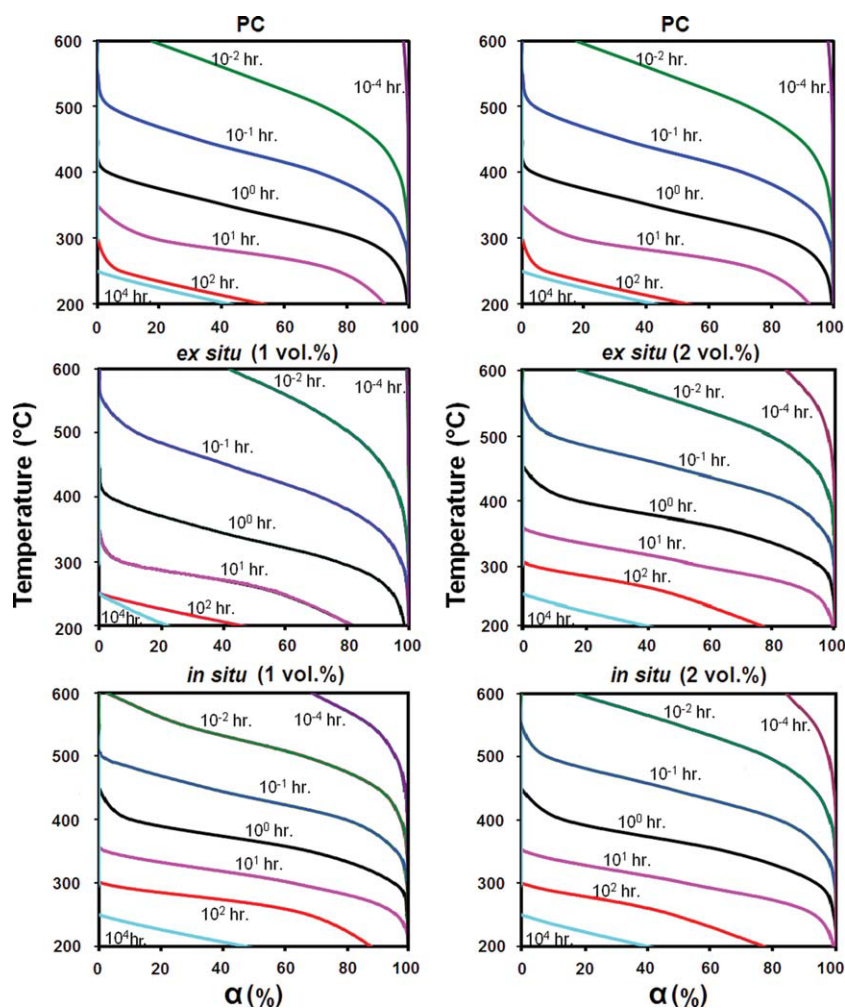


**Figure 8**  $\alpha$ - $t$ - $T$  plots for pure PC and Pd/PC nanocomposites with (a) 1 vol % and (b) 2 vol % Pd. [Color figure can be viewed in the online issue, which is available at [www.interscience.wiley.com](http://www.interscience.wiley.com).]

not considered due to its negligible contribution to the weight loss.

To start with, the  $T_i$  and  $T_f$  of the thermal degradation of nanocomposites are noted down from the TGA plots. Using these data, a new term called the work of decomposition ( $\Theta$ ) is calculated as follows,

$$-\int_1^\alpha \frac{d\alpha}{\alpha} = -\ln \alpha = \int_0^t k_0 \exp\left[-\frac{Q}{RT}\right] dt = k_0 \Theta \quad (7)$$

where

$$\Theta = \int_0^t \exp\left[-\frac{Q}{RT}\right] dt \quad (8)$$

As shown in eqs. (7) and (8), each curve is influenced by kinetic parameters of  $Q$  and  $k_0$ . Now, a single master curve of  $\alpha$  vs.  $\ln\Theta$  for a sample all four heating rates can be plotted. As shown in Figure 7 that, the decomposition sigmoid at all four heating

rates are merged down into one thereby developing the MDC. Minute differences in the MDC plots noticed might be due to the deviations/errors associated with the temperature and weight measurement and the calculation of  $Q$  and  $k_0$ .

#### Weight-temperature-temperature ( $\alpha$ - $t$ - $T$ ) Plots

For a given time ( $t$ ) under an isothermal condition at temperature ( $T$ ), the normalized weight ( $\alpha$ ) can be calculated using the following equation:

$$-\ln \alpha = k_0 \exp\left[-\frac{Q}{RT}\right] t \quad (9)$$

For a Pd/PC nanocomposite sample,  $k_0$  and  $Q$  can be calculated by the Kissinger method. The normalized weight-time-temperature ( $\alpha$ - $t$ - $T$ ) plots for the nanocomposites were constructed and are shown in the Figure 8. This  $\alpha$ - $t$ - $T$  plot helps in determining the allowable working conditions (time and temperature

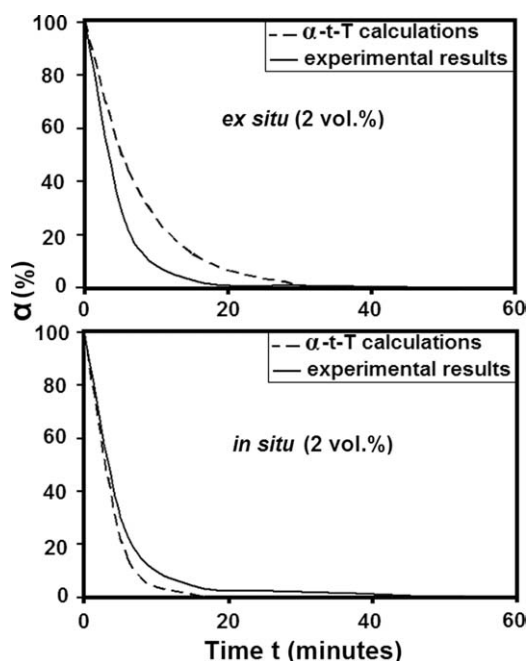


**Figure 9** Verification of calculations from  $\alpha$ - $t$ - $T$  plots with the isothermal measurements taken at 450°C for 2 vol % *ex situ* and *in situ* nanocomposites.

combination of exposure) for a given nanocomposite sample.<sup>31</sup>

The values obtained from  $\alpha$ - $t$ - $T$  plots were verified with the isothermal measurements for the samples. With the values of  $Q$  and  $k_0$  obtained from Table II, the  $\alpha$  can be back-calculated using eq. (9) for a given time and temperature combination. Isothermal measurements of both 1 and 2 vol % of the *ex situ* and *in situ* samples are in good agreement with the calculated values. For example, Figure 9 represents a comparison of calculated  $\alpha$  (at different time periods for the temperature of 450°C) during the degradation of 2 vol % *ex situ* and *in situ* samples with the  $\alpha$  obtained from the isothermal measurements. The differences noticed between the experimental and calculated  $\alpha$  values can be possibly reduced by narrowing the errors associated with the temperature and weight measurement and the  $Q$  and  $k_0$  calculations.

## CONCLUSIONS

Pd/PC nanocomposites were synthesized by two different techniques, *ex situ* and *in situ* methods. The Pd nanoclusters produced by the *ex situ* method were well-dispersed whereas the Pd nanoclusters produced by the *in situ* method were agglomerated. The influences of the heating rates, Pd content, and mode of synthesis on the thermal stability of the Pd/PC nanocomposites were investigated. The thermal degradation of the PC in Pd/PC nanocompo-

sites was found to follow first-order reaction kinetics. We found that the *ex situ* and *in situ* Pd/PC nanocomposites had enhanced thermal stability by investigating the temperature response for the onset of degradation, the maximum decomposition rate, the end of degradation, and the overall degradation time. Further, differences were noted in the activation energies  $Q$  and rate constant parameter  $k_0$  for the degradation of the PC and the Pd/PC nanocomposites as calculated via the Kissinger method. Master decomposition curve (MDC) and weight-time-temperature ( $\alpha$ - $t$ - $T$ ) plots were developed to predict the dependency of thermal degradation of the PC in the Pd/PC nanocomposites on the time-temperature combinations. Decomposition analysis of the PC in the Pd/PC nanocomposite samples at isothermal conditions were used to validate the  $\alpha$ - $t$ - $T$  plots within reasonable agreement.

## References

1. Carolyn, M.; Sih, B. C.; Scott, T. L.; Wolf, M. O. *J Mater Chem* 2005, 15, 2433.
2. Athawale, A. A.; Bhagwat, S. V.; Katre, P. P. *Sens Actuators B: Chem* 2006, 114, 263.
3. Houdayer, A.; Schneider, R.; Billaud, D.; Ghanbaja, J. *J Appl Organomet Chem* 2005, 19, 1239.
4. Atre, S. V.; Valmikanathan, O. P.; Meka, D. B.; Prasad, S. *Nanotech* 2008, 1, 794.
5. Xia, X.; Cai, S.; Xie, C. *Mater Chem Phys* 2006, 95, 122.
6. Chattopadhyay, S.; Datta, A. *Synth Met* 2005, 155, 365.
7. Aymonier, C.; Bortzmeyer, D.; Thomann, R.; Mulhaupt, R. *Chem Mater* 2003, 15, 4874.
8. Liu, F. K.; Hsieh, S. Y.; Ko, F. H.; Chu, T. C. *Colloids Surf A: Physicochem Eng Aspects* 2002, 231, 31.
9. Hsu, S. H.; Chou, C. W.; Tseng, S. M. *Macromol Mater Eng* 2004, 289, 1096.
10. Peng, Z.; Kong, L. X.; Li, S. D.; Spiridonov, P. *J Nanosci Nanotech* 2006, 6, 3934.
11. Gole, A.; Murphy, C. J. *Chem Mater* 2005, 17, 1325.
12. Akamatsu, K.; Takei, S.; Mizuhata, M.; Kajinami, A.; Deki, S.; Takeoka, S.; Fuji, M.; Hayashi, S.; Yamamoto, K. *Thin Film Solids* 2000, 359, 55.
13. Sarma, T. K.; Chowdhury, D.; Paul, A.; Chattopadhyay, A. *Chem Commun* 2002, 10, 1048.
14. Briemer, M. A.; Yevgeny, G.; Sy, S.; Sadik, O. A. *Nano Lett* 2001, 1, 305.
15. Brust, M.; Walker, M.; Bethell, M.; Schiffrin, D.; Whyman, D. J. *J Chem Soc Chem Commun* 1994, 20, 801.
16. Atre, S. V.; Valmikanathan, O. P.; Pillai, V. K.; Mulla, I. S.; Ostroverkhova, O. *NSTI Nanotech Conf Trade Show* 2007, 1, 158.
17. Zamborini, F. P.; Gross, S. M.; Murray, R. W. *Langmuir* 2001, 17, 481.
18. Sun, Y.; Frenkel, A. I.; Isseroff, R.; Shonbrun, C.; Forman, M.; Shin, K.; Koga, T.; White, H.; Zhang, L.; Zhu, Y.; Rafailovich, M. H.; Sokolov, J. C. *Langmuir* 2006, 22, 807.
19. Koga, K.; Ikeshoji, T.; Sugawara, K. *Phys Rev Lett* 2004, 92, 11507.
20. Chen, M.; Falkner, J.; Guo, W. H.; Zhang, J. Y.; Sayes, C.; Colvin, V. L. *J Colloid Interface Sci* 2005, 287, 146.
21. Jewrajka, S. K.; Chatterjee, U. *J Polym Sci Part A: Polym Chem* 2006, 44, 1841.

22. Khanna, P. K.; Singh, N.; Charan, S.; Subbarao, V. V. S.; Gokhale, R.; Mulik, U. P. *Mater Chem Phys* 2005, 93, 117.
23. Wang, J.; Montville, D.; Gonsalves, K. E. *J Appl Polym Sci* 1999, 72, 1851.
24. Henglein, A.; Giersig, M. *J Phys Chem B* 1999, 103, 9533.
25. Lee, J. Y.; Liao, Y.; Naghata, R.; Horiuchi, S. *Polymer* 2006, 47, 7970.
26. Huang, H. M.; Chang, C. Y.; Liu, I. C.; Tsai, H. C.; Lai, M. K.; Tsiang, C. C. R. *J Polym Sci Part A: Polym Chem* 2005, 43, 4710.
27. Krkljes, A. N.; Marinovic-Cincovic, M. T.; Kacarevic Popovic, Z. M.; Nedeljkovic, J. M. *Thermochim Acta* 2007, 460, 28.
28. Kissinger, H. E. *Anal Chem* 1957, 29, 1702.
29. Polli, H.; Pontes, L. A. M.; Souza, M. J. B.; Fernandes, V. J., Jr.; Araujo, A. S. *J Therm Anal Calorimetry* 2006, 86, 469.
30. Diantonio, C. D.; Ewsuk, K. G.; Bencoe, D. *J Am Cer Soc* 2005, 88, 2722.
31. Aggarawal, G.; Park, S. J.; Smid, I.; German, R. M. *Metall Mater Trans A* 2007, 38, 606.